Photodiagnosis and Photodynamic Therapy 23 (2018) 1–8

Contents lists available at ScienceDirect

Photodiagnosis and Photodynamic Therapy

journal homepage: www.elsevier.com/locate/pdpdt

Cell death mechanisms in *Leishmania amazonensis* triggered by methylene blue-mediated antiparasitic photodynamic therapy

Débora P. Aureliano[a], José Angelo Lauletta Lindoso[b,c,d], Sandra Regina de Castro Soares[d], Cleusa Fumika Hirata Takakura[e], Thiago Martini Pereira[f], Martha Simões Ribeiro[a,*]

[a] Center for Lasers and Applications, IPEN-CNEN/SP, São Paulo, SP, Brazil
[b] Laboratório de Investigação Médica (LIM 38), Hospital das Clínicas, Faculdade de Medicina (HCFMUSP), Universidade de São Paulo, São Paulo, SP, Brazil
[c] Instituto de Medicina Tropical, Universidade de São Paulo, São Paulo, SP, Brazil
[d] Instituto de Infectologia Emilio Ribas-SES-SP, São Paulo, SP, Brazil
[e] Faculdade de Medicina (FMUSP), Universidade de São Paulo, São Paulo, SP, Brazil
[f] Universidade Federal de São Paulo (UNIFESP), Departamento de Ciência e Tecnologia, São José dos Campos, SP, Brazil

ARTICLE INFO

Keywords:
Apoptosis
Flow cytometry
Membrane fluidity
Membrane potential
Microscopy
Photodynamic therapy
Cutaneous leishmaniasis

ABSTRACT

Antiparasitic photodynamic therapy (ApPDT) is an emerging approach to manage cutaneous leishmaniasis (CL) since no side effects, contraindications and parasite resistance have been reported. In addition, methylene blue (MB) is a suitable photosensitizer to mediate ApPDT on CL. In this study we aimed to look for the best parameters to eradicate *Leishmania amazonensis* and investigated the cell death pathways involved in MB-mediated ApPDT. MB uptake by parasites was determined using different MB concentrations (50, 100, 250 and 500 μM) and incubation times (10, 30 and 60 min). *L. amazonensis* promastigotes were cultured and submitted to ApPDT using different concentrations of MB (50, 100 and 250 μM) combined to a red LED emitting at 645 ± 10 nm. The pre-irradiation time was 10 min. Two optical powers (100 mW and 250 mW) were tested and cells were exposed to 60 and 300 s of MB-mediated ApPDT delivering energies of 6, 15, 30 and 75 J and fluences of 21.2, 53.1, 106.2 and 265.4 J/cm^2, respectively. Following ApPDT, cells were prepared for flow cytometry and transmission electron microscopy to unravel the mechanisms of cell death. Our results showed the lowest MB concentration (50 μM) and the lowest optical power (100 mW) promoted the highest percentage of cell decrease. ApPDT caused alterations on cell membrane permeability as well depolarization of mitochondrial membrane potential. We also observed ultrastructural changes of the parasites such as cell shrinkage, intense vacuolization of the cytoplasm, enlargement of mitochondrion-kinetoplast complex, and small blebs on parasite flagella and cell membrane after MB-mediated ApPDT. Taken together, our findings ratify that ApPDT parameters play a pivotal role in cell susceptibility and suggest that apoptosis is involved in parasite death regardless MB-mediated ApPDT protocol.

1. Introduction

Leishmaniasis is an infectious disease caused by species of protozoa of the *Leishmania* genus that is transmitted by phlebotomine sand flies. Despite the variety of clinical manifestations, the most common form is cutaneous leishmaniasis (CL) following visceral leishmaniasis and mucosal leishmaniasis. Nowadays, leishmaniasis is endemic in at least 97 nations and territories, and there are over one million cases per year. More than 87% of the cases are reported in Africa, Middle West and Latin America, mainly in Brazil. Despite the large number of cases, this disease is still considered neglected since it affects mainly underprivileged people and is predominant in tropical and subtropical regions. In addition, leishmaniasis has also demanded attention in nonendemic areas due to the high number of international travelers [1–3].

Current treatments for leishmaniasis are based on the use of pentavalent antimonials, amphotericin B, pentamidine and miltefosine. However, these drugs present many limitations of use related to safety, stability, resistance, high cost, long-term treatment and difficulty of application. Moreover, they cause critical side effects such as nephrotoxicity, hepatotoxicity, cardiotoxicity and arthralgia besides the contraindications to pregnancy and heart, renal or hepatic failure [3,4].

In this context, photodynamic therapy (PDT) or antiparasitic photodynamic therapy (ApPDT) is a promising approach for leishmaniasis.

* Corresponding author at: Center for Lasers and Applications, Av. Prof. Lineu Prestes, 2242, Cidade Universitária, CEP: 05508-000, São Paulo, SP, Brazil.
E-mail address: marthasr@usp.br (M.S. Ribeiro).

https://doi.org/10.1016/j.pdpdt.2018.05.005
Received 23 October 2017; Received in revised form 19 March 2018; Accepted 7 May 2018
Available online 08 May 2018
1572-1000/

PDT is based on the damage of cells by light-induced reactions called photosensitization that occurs when photosensitizer (PS) absorbs light and transfers its energy to neighboring molecules generating reactive oxygen species (ROS), which induce cell death by oxidative stress. Due to its action mechanism, no reports about resistance and toxicity are described [5].

Currently, literature is rich about the use of ApPDT on leishmaniasis both in vitro and in vivo using different PS structures such as porphyrins, curcuminoids, phthalocyanines, anthraquinones, phenothiazines and others [6–9]. Authors have reported successful outcome depending on type and concentration of PS, light parameters and *Leishmania* species. Recently, Pinto and coworkers showed that methylene-blue (MB)-mediated ApPDT was able to inactivate and induce significant morphological changes in *Leishmania* promastigotes [9].

In fact, due to its photochemical and photophysical characteristics, MB has been commonly used to mediate PDT of bacteria, fungi and parasites. It is synthetic, water soluble and cost-effective PS that accumulates in the target microorganism rather than host cells triggering efficient microbial reduction under red light. Despite its large use in ApPDT, no studies about its biological effects on *Leishmania* spp. are reported.

In this work, we explored the mechanisms of cell death involved in methylene blue (MB)-mediated ApPDT on *Leishmania (Leishmania) amazonensis* promastigotes. *L. amazonensis* is a suitable model since it is an etiological agent responsible for the development of CL, severe diffuse cutaneous leishmaniasis and even visceral leishmaniasis. Firstly, we used different concentrations of MB and distinct incubation times to verify MB uptake by the parasite cells and establish the pre-irradiation time. After, we associated MB to distinct light parameters to identify the best protocols for parasite inactivation by MTT viability assay. Lastly, we used flow cytometry and transmission electron microscopy (TEM) to investigate the plasma membrane permeability, membrane potential, and ultrastructural changes in order to unravel the cell death pathways.

2. Materials and methods

2.1. Parasites

L. amazonensis promastigotes (MHO/BR/73/M2269) were cultured in M199 medium (Sigma-Aldrich, USA) supplemented with fetal bovine serum (FBS), HEPES, penicillin and streptomycin antibiotics at 26 °C for 4–7 days. For the experiments, we used 10^7 parasites/ml [10].

2.2. Uptake assay

Cells were cultured as described previously. A stock solution of MB (Sigma-Aldrich, USA) was prepared in distilled water at a concentration of 10 mM. This solution was diluted in phosphate-buffered saline (PBS) in concentrations of 50, 100, 250 and 500 μM and cells were incubated with MB during 10, 30 and 60 min in the dark. Thereafter, cells were centrifuged at 2100*g* for 10 min, washed copiously with PBS and centrifuged again. Then, the pellets were suspended in 1 ml 0.1 M NaOH and 1% sodium lauryl sulfate (SLS) for 24 h. The fluorescence was measured at spectrometer (Spectra MAX, Gemini EM, Molecular Devices, USA) at excitation of λ = 532 nm and emission of λ = 690 nm. The assay was performed in triplicate at four different days (n = 12).

2.3. Antiparasitic photodynamic therapy

For ApPDT, we used MB in concentrations of 50, 100, and 250 μM and a LED device (LED630, MMOptics, Brazil) emitting at λ = 645 nm ± 10 nm. Two different optical powers (100 and 250 mW) were used with two distinct exposure times (60 and 300 s) delivering energies of 6, 15, 30 and 75 J. The pre-irradiation time was 10 min determined by the uptake assay. Samples were placed in wells of a 96-well plate, at least two-well spaced, and individually irradiated from bottom upwards. A black mask was specially projected to cover the plate and avoid irradiated light in the neighboring wells. The light beam was adjusted to the diameter of 0.6 cm corresponding to the bottom of the well. Thus, we used fluences of approximately 21.2, 53.1, 106.2 and 265.4 J/cm^2 depending on power and exposure time tested (Table 1). Assays were performed in triplicate at four different days (n = 12).

Table 1
Light parameters used in MB-mediated ApPDT of *L. amazonensis*.

Power (mW)	Exposure time (s)	Energy (J)	Fluence (J/cm^2)
100	60	6	21.2
250	60	15	53.1
100	300	30	106.2
250	300	75	265.4

2.4. Cell viability by colorimetric MTT assay

Immediately after ApPDT, 25 μl of MTT solution (5 mg/ml) in PBS followed by syringe filtration was added to each well and incubated at 26 °C for 3 h. After incubation, samples were centrifuged (2100*g*, 10 min, 22 °C) and supernatant was removed. Thereafter, one hundred-μl of pure DMSO was added for homogenization and formazan solubilization [11]. After shaking of 15 min, the readings were recorded as absorbance at 570 nm (reference filter 630 nm) on a microplate reader (Multiskan MCC/340, USA). Control samples were untreated promastigotes. Relative number of viable promastigotes was determined by the optical absorbance using the equation:

$$Cell\ Viability = (OD_T - OD_B)/(OD_C - OD_B) \times 100$$

where OD_B, OD_C, OD_T are the optical density of blank, untreated control and treated samples, respectively [12].

2.5. Cytofluorimetric measurements

Parasites were incubated with annexin V conjugated with fluorescein isothiocyanate (FITC) and propidium iodide (PI) for 15 min protected from light according to the kit information annexin V for FITC apoptosis detection (eBioscience, USA). Samples were excited at λ = 488 nm and fluorescence was detected at λ = 525 nm (FITC emission) and λ = 575 nm (PI emission). Cells were identified by flow cytometry and divided into four quadrants: Q1: - annexin V + PI; Q2: + annexin V + PI; Q3: + annexin V - PI and Q4: - annexinV - PI. Ten thousand independent events were recorded and standardized for all tests.

To investigate mitochondrial membrane depolarization, parasites were washed with cold PBS 0.01 M, pH 7.2, suspended in 0.5 ml of the reagent JC-1 (5,5′,6,6′-tetrachloro-1,1′,3,3′-tetraethylbenzimidazolylcarbocyanine iodide) and incubated at 37 °C for 15 min. After, cells were centrifuged for 10 min at 2100 *g* and the supernatant was removed. The pellet was resuspended in 2 ml assay buffer (1X, JC-1 kit), twice centrifuged, the supernatant was discarded and resuspended again in 0.5 ml of assay buffer (1X, JC-1 kit). JC-1 is a cyanine dye that is a monomer at low concentrations, but forms J-aggregates at higher concentrations. Thus, the fluorescence of JC-1 makes possible the discrimination of energized (orange/red fluorescence) and deenergized (green fluorescence) mitochondria in *Leishmania*. The detection of the mitochondrial membrane electric potential (Δψm) was analyzed in ten thousand independent events using a laser emitting at λ = 488 nm and emitted fluorescence was collected at λ = 527 nm for JC-1 monomers and λ = 590 nm for J-aggregates.

2.6. Ultrastructural analysis

Alterations in the ultrastructure of the parasites were analyzed by

TEM. *L. amazonensis* promastigotes were washed five times with PBS and fixed with glutaraldehyde solution (3% glutaraldehyde in 0.1 M sodium cacodylate buffer containing 0.1 M sucrose, pH 7.4) at 4 °C for 30 min. The samples were post-fixed in a mixture of 1% phosphate-buffered osmium tetroxide and 1.5% potassium ferrocyanide for 1 h prior to dehydration in a graded ethanol series and embedding in a propylene oxide-Epon sequence (PolyBed 812, Poly-sciences, USA). Sections of 80 nm-thickness were cut using a diamond knife on an ultramicrotome (Reichert Ultracut UCT, Leica, Germany).The electron-micrographs were obtained using an electron microscope JEM1010 (Jeol, USA).

2.7. Statistical analysis

For uptake and cell viability assays, calculations were carried out using GraphPad Prism 5 software. Data were checked regarding normality by Shapiro-Wilk test and compared using one-way analysis of variance (ANOVA). Tukey test was used as a post-test to identify statistically significant differences among groups. Results were considered as statistically significant when $p < 0.05$.

3. Results

We verified that MB uptake by parasites was mostly dependent on MB concentration. The highest concentrations (250 and 500 μM) showed higher uptakes, about 1×10^8 molecules/parasite, with no statistically significant difference detected between them. In addition, no statistically significant differences were observed comparing 10, 30 and 60 min of incubation regardless MB concentration (Fig. 1). Thus, we proceeded with the cell viability assays incubating parasites with 50, 100, and 250 μM of MB for 10 min before irradiation.

Regarding cell viability, light groups were similar to untreated control (about 95% of cell viability) regardless the optical power (100 mW or 250 mW) during 300 s. In comparison, we observed MB in all tested concentrations reduced viability about 20%, however, there was no statistically significant difference compared to untreated control (Figs. 2 and 3).

When MB was used at 50 μM associated to LED (100 mW) and energies of 6 J and 30 J we observed significant reduction of viability in approximately 55% for 60 s and 80% for 300 s while 100 μM MB significantly inactivated about 30% and 80% of parasites for 60 and 300 s, respectively. When ApPDT was performed using MB at 250 μM, we only observed a statistically significant difference compared to control at 300 s of irradiation (30 J of energy) (Fig. 2).

On the other hand, a higher LED output power (250 mW) showed significant cell viability decrease for all MB concentrations tested

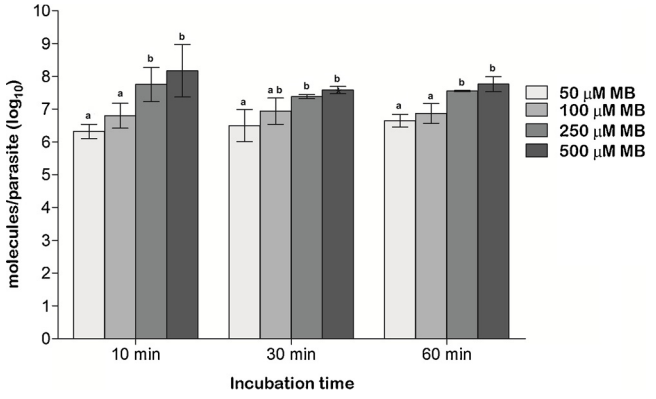

Fig. 1. Mean values of MB uptake of *L. amazonensis* promastigotes (n = 12) expressed as molecules/parasite (log10). Black bars indicate the standard error of the results. Different letters indicate statistically significant differences ($p < 0.05$).

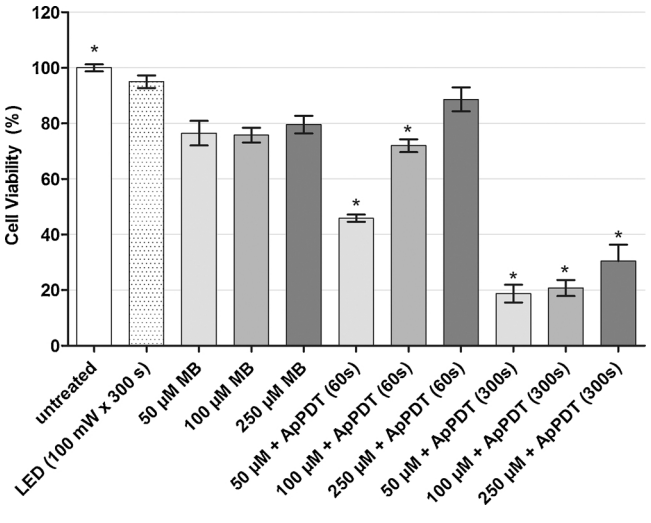

Fig. 2. Mean values of cell viability of *L. amazonensis* promastigotes (n = 12) with LED of 100 mW. Black bars indicate the standard error of the results. * indicate statistically significant differences compared to untreated control ($p < 0.05$).

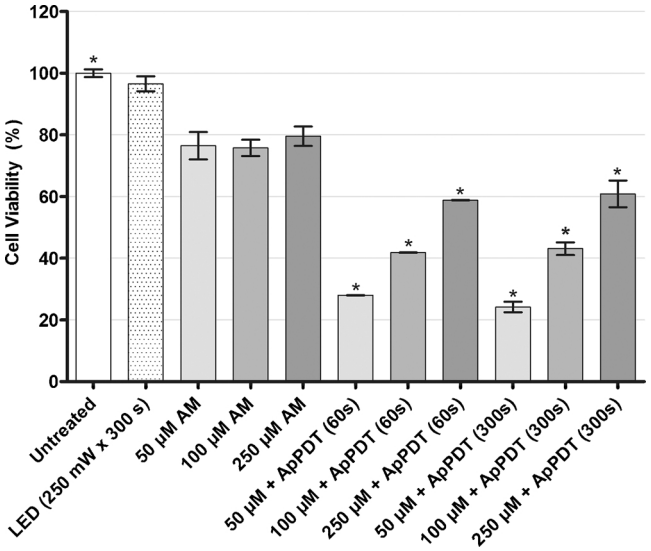

Fig. 3. Mean values of the cell viability of *L. amazonensis* promastigotes (n = 12) with LED of 250 mW. Black bars indicate the standard error of the results. * indicate statistically significant differences compared to untreated control ($p < 0.05$).

(Fig. 3). Interestingly, parasite inactivation in this case was independent on exposure time. In addition, the lower MB concentration was more effective in reducing parasite viability. MB-mediated ApPDT at 50 μM reduced viability in 75%, 100 μM in 50% and 250 μM in about 40%.

Thereafter, we continued to investigate the cell death pathways involved in 50 μM and 100 μM MB-mediated ApPDT using 100 mW and 250 mW of red LED for 300 s (30 J and 75 J, respectively) to verify if PS concentration and light parameters could induce different responses on parasite death pathways.

The exposure of phosphatidylserine (PPS) permeability using annexin V vs PI is showed in Fig. 4. As expected, 100% of unmarked and untreated cells are in Q4 (Fig. 4A). On the other hand, it is known that *Leishmania* species express PPS so 35.7% of parasites are in Q3 (Fig. 4B). Also it is possible to notice that PI-stained cells expressing PPS (Q2) is about 3 times higher for LED 100 mW than LED 250 mW (30.5% x 13.3%, Fig. 4C and D). Regarding MB concentrations, similar cell

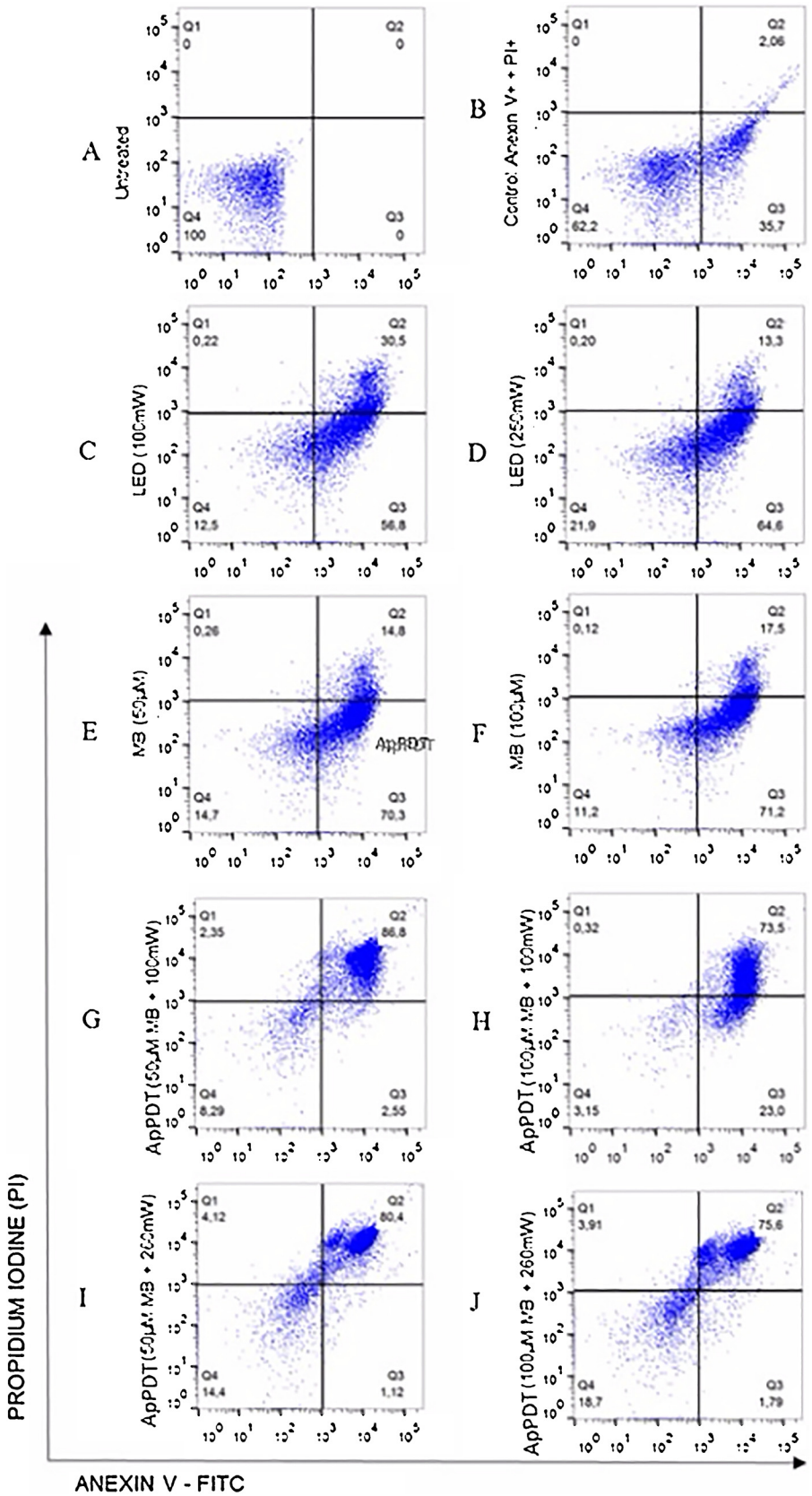

Fig. 4. Dot plot of the detection of exposure of PPS and membrane permeability in *L. amazonensis* promastigotes by Annexin V vs. PI. A: untreated and unmarked promastigotes; B: untreated promastigotes marked with Annexin V+ and. PI+; C and D: irradiated promastigotes using LED 100 mW and 250 mW, respectively; E and F: MB-stained promastigotes at concentrations of 50 µM and 100 µM, respectively; G and H: photoinactivated promastigotes following LED 100 mW and MB at 50 µM and 100 µM, respectively; I and J: photoinactivated promastigotes following LED 250 mW and MB at 50 µM and 100 µM, respectively.

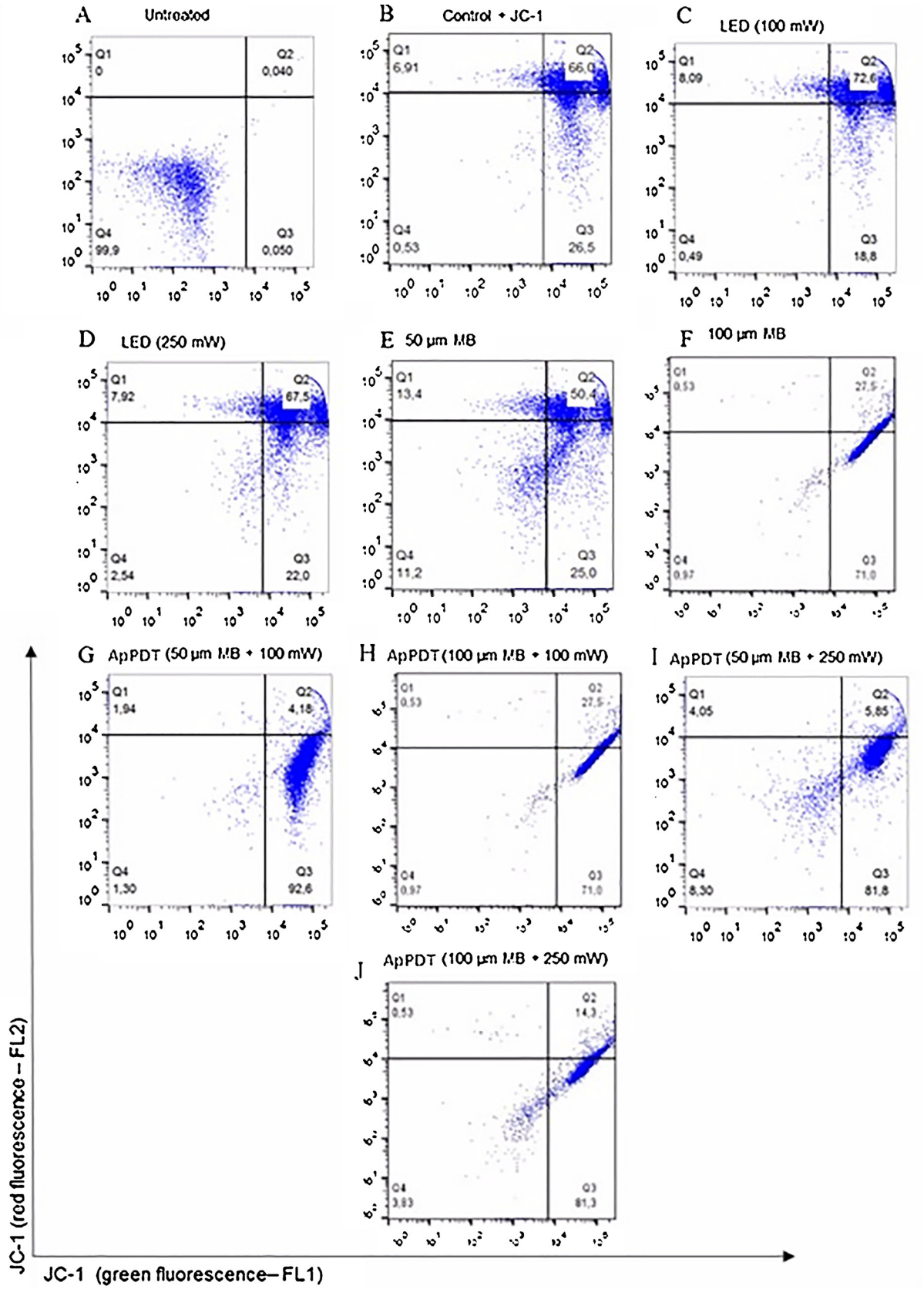

Fig. 5. Dot plot of mitochondrial membrane potential changes (Δψm) in *L. amazonensis* promastigotes by JC-1 staining. A: untreated and unmarked promastigotes; B: untreated and JC-1 marked promastigotes; C and D: irradiated promastigotes with LED 100 mW and 250 mW, respectively; E and F: MB-stained promastigotes at concentrations of 50 µM and 100 µM, respectively; G and H: photoinactivated promastigotes following LED 100 mW and MB at 50 µM and 100 µM, respectively; I and J: photoinactivated promastigotes following LED 250 mW and MB at 50 µM and 100 µM, respectively.

population was detected in Q2 (14.8% x 17.5%, Fig. 4E and F). Although cell population differs in the quadrants, observe that for MB and light groups the cloud behavior is very similar. In contrast, clouds were rather dissimilar following ApPDT. In fact, all ApPDT tested protocols showed a high percentage of non-viable cells in Q2 (> 70%) indicating late apoptosis phase or necrosis (Fig. 4G–J). Following 300 s of ApPDT, MB at 50 μM combined to LED 100 mW exhibited the highest percentage of cell death (88.6%) while 100 μM-MB associated to LED 100 mW showed the lowest percentage (73.5%).

Regarding mitochondrial membrane potential also as expected 99.9% of untreated and unmarked cells were in Q4 (Fig. 5A). Untreated and JC-1-marked cells as well as LED-irradiated promastigotes (Fig. 5B–D) presented both green and red fluorescence signals with higher cell population in Q2 (66% to 72.6%) indicating the presence of both cytoplasmic JC-1 monomer and mitochondrial J-aggregates in these cells. Concerning MB groups, intriguing results were observed. MB at 50 μM also showed higher cell population in Q2 (50.4%) but 100 μM-MB promoted mitochondrial deenergization since an increase of the intensity of the green fluorescence signal for 71% of cell population in Q3 was detected (Fig. 5E and F). Deenergized mitochondria, i.e., low mitochondrial respiratory activity, were also perceived following ApPDT. Regardless the protocols, ApPDT groups exhibited an intense green fluorescence signal since the highest percentage of cells was in Q3 (71%–92.6%, Fig. 5G–J). These findings corroborate an apoptotic cell death. Once again, the protocol 50 μM-MB and LED 100 mW induced to the highest number of green fluorescent cells (92.6%).

From previous assays, our results indicated that apoptosis is the main cell death pathway of *L. amazonensis* promastigotes regardless the ApPDT protocol. Thus, we evaluated changes in parasite ultrastructure following ApPDT parameters that promoted the highest parasite inactivation, i. e., 50 μM-MB and LED 100 mW.

Untreated promastigotes exhibited their characteristic elongate fusiform shape, a rounded nucleus in central position with peripherally condensed chromatin and mitochondrion with its typical highly elongate shape. The plasma membrane was intact. Well-preserved flagellar pocket and lipid bodies were also observed (Fig. 6A). MB-stained (Fig. 6B) or only irradiated parasites (Fig. 6C) also showed intact cell membrane and organelles as nucleus, mitochondria, and kinetoplast.

After ApPDT, we observed a significant change in internal and external morphology of the protozoan (Fig. 6D–F). Cells displayed several ultrastructural alterations characteristic of apoptotic cells. Promastigote cytoplasm seemed less electron dense, with intense cytoplasmic vacuolization and increase of lipid reservoirs. Parasite flagella became enlarged, flagellar pockets were disarranged with some vesicles, the nucleus exhibited dispersed chromatin, nuclear envelopes showed some laxity in their structure and the complex mitochondrion-kinetoplast was disintegrated and augmented with loss in matrix density. ApPDT also induced cell shrinkage and a rounded appearance of the promastigotes. Blebbing was perceived on parasite flagella and plasma membrane. No cell membrane detachment and autophagosomes were noticed.

4. Discussion

In this study we explored the leishmanicidal effects of different concentrations of MB associated to different light parameters to identify the cell death mechanisms involved in the inactivation of *L. amazonensis* promastigotes by ApPDT.

Firstly we observed that MB at 50 μM conducted to the highest leishmanicidal effect independent of irradiation protocol while 250 μM-MB caused the lowest inactivation. These findings were unpredictable since it is expected that the higher the number of molecules in a MB solution (i.e., high molarity) the greater the ROS production, as consequence, to induce photodamage on the cells. However, we could assume that high PS concentrations lead to an optical shielding avoiding the light penetration through the parasite suspension [13]. In addition, it is known that high concentrations and presence of cells promote MB aggregation, i.e., the dimer/monomer ratio tends to increase [14]. Thus, the maximum absorbance of the dye is modified and its effectiveness in the photodynamic action can be reduced.

Regarding light parameters, we perceived that 100 mW of red LED during 300 s was more effective than 60 s, that fits with other studies in literature [15]. In contrast, parasite inactivation was similar when we used 250 mW for both 60 s and 300 s. For the highest optical power, no further killing was detected when increasing the exposure time, and, consequently, the fluence. Despite contradictories, these data corroborate those reported by Prates et al., who demonstrated that fluence is not the major contributor for successful ApPDT [16].

The response to photodynamic action can occur in different cell types, such as mammal malignant cells, prokaryotes (bacteria), and lower eukaryotic ones, such as fungi and parasites [17,18]. Additionally, PS interacts with cells and its subcellular localization plays a pivotal role to initiate the death process following photodamage, which may be necrotic or by programmed pathways as autophagy or apoptosis. Thus, we investigated the possible death pathways of *L. amazonensis* promastigotes using flow cytometry to identify the mechanisms involved in MB-mediated ApPDT.

Annexin V has been used to detect apoptotic cells [19]. This is due to the loss of membrane asymmetry near the apoptosis phase [20]. In apoptotic cells, the phospholipid phosphatidylserine, a component of the cell membrane, is displaced from the inside to outside of the plasma membrane, with PPS exposure in the external environment. This modification of the cellular structure signalizes its death by apoptosis to the environment [19].

On the other hand, PI is very applied in flow cytometry to distinguish viable from non-viable cells [21]. Viable cells do not allow PI fluorochrome to enter the membrane while cells in process of late stage apoptosis allow the PI to enter their nuclei and bind to the DNA that has been cleaved because apoptotic process [21]. Thus, cells that are negative for annexin V and PI are viable, cells that are positive for annexin V and negative for PI are considered in early apoptosis, and cells that are positive for annexin V and PI are in late apoptosis or dead [19,21].

In our study, untreated cells naturally expressed PPS (about 35%). This finding was expected since a subpopulation of promastigote forms of *L. amazonensis* naturally expose PPS on their surface as part of the normal metacyclogenic process occurring in axenic cultures and gut of phlebotomines [22]. In addition, light or MB alone induced approximately 60% to 70% of cells to initial apoptosis phase. Apparently, cell exposure to light or MB caused some mechanism of self-protection or escape from these parasites. In fact, it has long been described that parasites of *Leishmania* genus can simulate apoptosis (apoptosis-like) to attract the macrophages of the immune system and be phagocytized. This situation is an altruistic mechanism of escape that these parasites possess to survive in stress situations [23]. Following ApPDT, promastigotes presented a high percentage (73% to 87% depending on ApPDT protocol) of non-viable cells that indicates a late apoptosis phase.

Late apoptosis was also observed by other authors using different leishmanicidal drugs such as tamoxifen, nitro-heterocyclic derivatives and ursolic acid [24–26]. Those studies concluded that late apoptosis in *Leishmania* parasites is not reversible. This is an important factor for the effectiveness of MB-mediated ApPDT and our study showed higher percentage of annexin V and PI-stained cells regardless the ApPDT protocol.

Thereafter, we evaluated the mitochondrial membrane potential by JC-1 fluorochrome. Promastigotes irradiated showed similar behavior to untreated cells indicating that only red LED 100 mW or 250 mW for 300 s did not promote any alteration in $\Delta\Psi_m$. Also MB at 50 μM for 10 min did not cause drastic change in $\Delta\Psi_m$. In contrast, 100 μM-MB and ApPDT altered the fluorescence distribution pattern suggesting mitochondrion deenergization, which is indicative of apoptotic cell death in the late stage, corroborating the previous results. Cell population exhibiting depolarization was about 71%–93% depending on ApPDT protocol. This finding could be explained by the high chemical

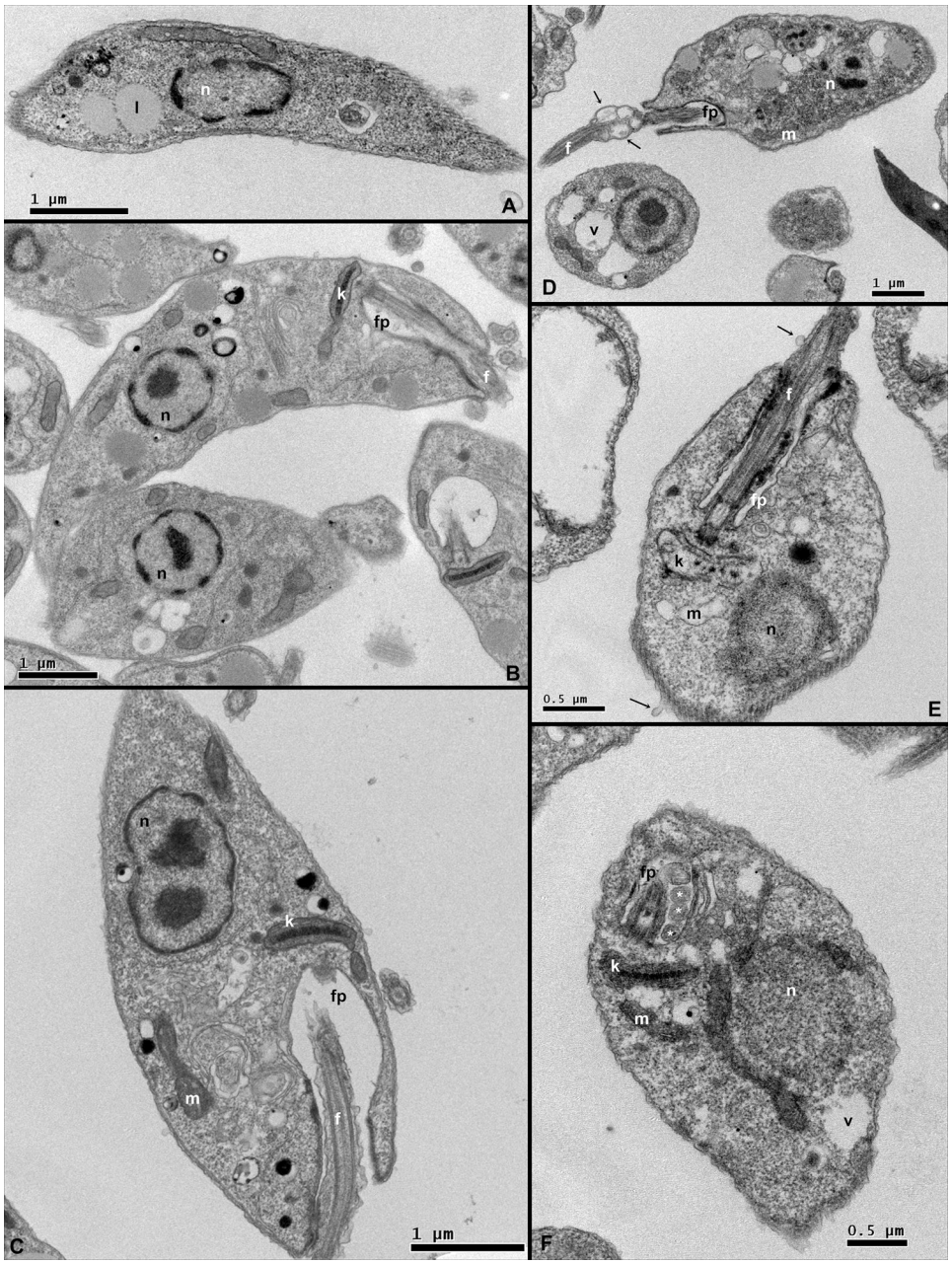

Fig. 6. Electron-micrographs of *L. amazonensis* promastigotes. A: untreated promastigote; B: irradiated promatisgote with LED 100 mW; C: 50 µM-MB-stained promastigote; D–F: photoinactivated promastigotes (50 µM-MB with LED 100 mW). Notice mitochondria-kinetoplast complex deformation and nucleus disorganization (D–F), vacuoles in the cytoplasm (D, F), and flagellar pocket enlargement with vesicle formation (F). Arrows point to blebs in the flagellum (D) and cell membrane (E). Note also the loss of cell membrane integrity but not its rupture. n - nucleus; m - mitochondrion; k - kinetoplast; f - flagellum; fp – flagellar pocket; v – vacuole, l – lipids, * - vesicle.

affinity of MB, a cationic PS, with negatively charged mitochondria [27,28].

Taken together, data obtained from flow cytometry suggest that apoptosis is involved in MB-mediated ApPDT. However, studies have described that the apoptotic death encompasses the change in the cellular form [19]. This change is always related to shrinkage, more specifically the reduction of cell size.

The ultrastructural analysis showed that untreated and light or MB-stained parasites preserved their morphological characteristics as intact membrane and internal organelles. After ApPDT, we observed significant changes in their ultrastructure. The parasite became rounded demonstrating cell retraction. This probably occurred due to loss of cytoskeletal integrity, a consequence for the cell that is unable to maintain its original elongate shape because the chain of apoptotic signals is triggered. Another study in literature described this same process of cytoskeletal disorganization in eukaryotic unicellular organisms during the programmed death process [19].

The cell membrane showed no rupture of its structure although localized perturbations caused membrane blebbing. Formation of blebs is a typical morphological feature of apoptosis [29]. In fact, the first visible characteristic of apoptotic morphologies is the cell rounding. After cell rounding, apoptotic membrane blebbing initiates, which includes the formation of circular protrusions at the plasma membrane [29].This finding could be explained by the peroxidation of lipids and proteins provoked by ApPDT, since that MB binds close to the double bonds in the alkyl chains favoring singlet oxygen production [30]. However, due to characteristics as tendency of aggregation, hydrophilicity, molecular geometry, and singlet oxygen decay, MB was not able to promote membrane rupture [31].

Regarding internal ultrastructures, we observed an intense vacuolization of the cytoplasm, retracted flagellar pockets, nucleus showed dispersed chromatin condensation to the margins, and nuclear envelopes presented some looseness in their structure. In addition, mitochondria presented disorganization in their internal lamellae, disarrangement along their length and the complex mitochondrion-kinetoplast became enlarged supporting our previous results, where

changes in mitochondrial membrane potential after ApPDT were verified. Indeed, some electron lucent structures observed by TEM may comprise damaged mitochondria (see Fig. 6E), which showed loss in matrix density. Mitochondrial injury was expected since a depolarization of the mitochondrial membrane potential was noticed following JC-1 assay. Interestingly, *Leishmania* spp. only have one mitochondrion, making this organelle a potential target for drugs, e.g., MB. As previously reported, MB has high affinity for mitochondria. Thus, the excessive oxidative stress generated by ApPDT was the starting point for triggering the programmed cell death, which is followed by mitochondrial dysregulation, a paramount feature of apoptosis [32]. These findings ratify those reported in literature about the action of leishmanicidal drugs [19,21,33–34] besides also indicating an apoptotic pathway for MB-mediated ApPDT.

For cancer cells literature reports that both apoptosis and autophagy could be involved in cell death by photodynamic treatment. However, for *Leishmania* parasites studies are scarce. This work was a first attempt to understand the cell death pathways of *Leishmania* promastigotes following MB-mediated ApPDT. Regardless ApPDT protocols used in this work, our results suggest that apoptosis is implicated in parasite death. Cell death by apoptosis could induce minimal inflammation and faster patient recovery. We hope this study provides scientific background and encourages future studies using MB-mediated ApPDT as a treatment for cutaneous leishmaniasis.

Acknowledgements

This work was supported in part by Institute of Photonics (INCT-573916/2008) from the Conselho Nacional de Desenvolvimento Científico e Tecnológico (CNPq). D. P. Aureliano also thanks CNPq for her scholarship.

References

[1] World Health Organization (WHO), Global Observatory on Health R&D, Preliminary analysis for R&D for leishmaniasis, version 16 Jan. 2017, 9 p.
[2] H. Goto, J.A. Lauletta Lindoso, Cutaneous and mucocutaneous leishmaniasis, Infect. Dis. Clin. North. Am. 26 (2012) 293–307, http://dx.doi.org/10.1016/j.idc.2012.03.001.
[3] C.V. David, N. Craft, Cutaneous and mucocutaneous leishmaniasis, Dermatol. Ther. 22 (2009) 491–502, http://dx.doi.org/10.1111/j.1529-8019.2009.01272.x.
[4] E. Torres-Guerrero, M.R. Quintanilla-Cedillo, J. Ruiz-Esmenjaud, R. Arenas, Leishmaniasis: a review, F1000Research 6 (2017) 750, http://dx.doi.org/10.12688/f1000research.11120.1.
[5] D.P. Aureliano, M.S. Ribeiro, J. Angelo, L. Lindoso, F.C. Pogliani, F.P. Sellera, D. Song, M.S. Baptista, Treatment and control of leishmaniasis using photodynamic therapy, in: D.M. Claborn (Ed.), Leishmaniasis - Trends Epidemiol. Diagnosis Treat. INTECH, 201410577257456.
[6] D.M. Souza, P.M. Alves, M.L.F. Silva, T.P. Paulino, H.O. Coraspe, M.M.S. Mendonça, B.M. Ribeiro, M.V. da Silva, V. Rodrigues Júnior, D.B.R. Rodrigues, 5-ALA-mediated photodynamic therapy reduces the parasite load in mice infected with *Leishmania braziliensis*, Parasite Immunol. (2017), http://dx.doi.org/10.1111/pim.12403.
[7] J.G. Pinto, L.C. Fontana, M.A. de Oliveira, C. Kurachi, L.J. Raniero, J. Ferreira-Strixino, In vitro evaluation of photodynamic therapy using curcumin on Leishmania major and Leishmania braziliensis, Lasers Med. Sci. 31 (2016) 883–890, http://dx.doi.org/10.1007/s10103-016-1928-5.
[8] A. Montoya, A. Daza, D. Muñoz, K. Ríos, V. Taylor, D. Cedeño, I.D. Vélez, F. Echeverri, S.M. Robledo, Development of a novel formulation with hypericin to treat cutaneous leishmaniasis based on photodynamic therapy in in vitro and in vivo studies, Antimicrob. Agents Chemother. 59 (2015) 5804–5813, http://dx.doi.org/10.1128/AAC.00545-15.
[9] J.G. Pinto, J.F.S. Martins, A.H.C. Pereira, J. Mittmann, L.J. Raniero, J. Ferreira-Strixino, Evaluation of methylene blue as photosensitizer in promastigotes of Leishmania major and Leishmania braziliensis, Photodiagn. Photodyn. Ther. 18 (2017) 325–330, http://dx.doi.org/10.1016/j.pdpdt.2017.04.009.
[10] F.L. Schuster, J.J. Sullivan, Cultivation of clinically significant hemoflagellates, Clin. Microbiol. Rev. 15 (2002) 374–389, http://dx.doi.org/10.1128/CMR.15.3.374-389.2002.
[11] R.C. Zauli-Nascimento, D.C. Miguel, J.K.U. Yokoyama-Yasunaka, L.I.A. Pereira, M.A. Pelli de Oliveira, F. Ribeiro-Dias, M.L. Dorta, S.R.B. Uliana, In vitro sensitivity of Leishmania (Viannia) braziliensis and Leishmania (Leishmania) amazonensis Brazilian isolates to meglumine antimoniate and amphotericin B, Trop. Med. Int. Health 15 (2010) 68–76, http://dx.doi.org/10.1111/j.1365-3156.2009.02414.x.
[12] S. Khademvatan, N. Adibpour, A. Eskandari, S. Rezaee, M. Hashemitabar, F. Rahim, In silico and in vitro comparative activity of novel experimental derivatives against Leishmania major and Leishmania infantum promastigotes, Exp. Parasitol. 135 (2013) 208–216, http://dx.doi.org/10.1016/j.exppara.2013.07.004.
[13] S. Núñez, A. Garcez, I. Kato, Effects of ionic strength on the antimicrobial photodynamic efficiency of methylene blue, Photochem. Photobiol. Sci. 13 (2014) 595–602, http://dx.doi.org/10.1039/c3pp50325a.
[14] M.N. Usacheva, M.C. Teichert, M.A. Biel, The role of the methylene blue and toluidine blue monomers and dimers in the photoinactivation of bacteria, J. Photochem. Photobiol. B 71 (2003) 87–98, http://dx.doi.org/10.1016/j.jphotobiol.2003.06.002.
[15] R.A. Prates, B.B. Fuchs, K. Mizuno, Q. Naqvi, I.T. Kato, M.S. Ribeiro, E. Mylonakis, G.P. Tegos, M.R. Hamblin, Effect of virulence factors on the photodynamic inactivation of cryptococcus neoformans, PLoS One 8 (2013) e54387, , http://dx.doi.org/10.1371/journal.pone.0054387.
[16] R.A. Prates, E.G. Silva, A.M. Yamada, L.C. Suzuki, C.R. Paula, M.S. Ribeiro, E.G. da Silva, A.M. Yamada Jr, L.C. Suzuki, C.R. Paula, M.S. Ribeiro, Light parameters influence cell viability in antifungal photodynamic therapy in a fluence and rate fluence-dependent manner, Laser Phys. 19 (2009) 1038–1044, http://dx.doi.org/10.1134/S1054660X09050284.
[17] M.R. Hamblin, Antimicrobial photodynamic inactivation: a bright new technique to kill resistant microbes, Curr. Opin. Microbiol. 33 (2016) 67–73, http://dx.doi.org/10.1016/j.mib.2016.06.008.
[18] T.K. Horne, M.J. Cronje, Cancer tissue classification, associated therapeutic implications and PDT as an alternative, Anticancer Res. 37 (2017) 2785–2807, http://dx.doi.org/10.21873/anticanres.11630.
[19] A. Jiménez-Ruiz, J.F. Alzate, E.T. Macleod, C.G.K. Lüder, N. Fasel, H. Hurd, Apoptotic markers in protozoan parasites, Parasites Vectors 3 (104) (2010), http://dx.doi.org/10.1186/1756-3305-3-104.
[20] A. Grivicich, I. Regner, A. da Rocha, Morte celular por apoptose, Rev. Bras. Cancerol. 53 (2007) 335–343 in portuguese.
[21] L. Galluzzi, S.A. Aaronson, J. Abrams, E.S. Alnemri, D.W. Andrews, E.H. Baehrecke, et al., Guidelines for the use and interpretation of assays for monitoring cell death in higher eukaryotes, Cell Death Differ. 16 (2009) 1093–1107, http://dx.doi.org/10.1038/cdd.2009.44.
[22] J.L. Wanderley, L.H. Pinto da Silva, P. Deolindo, L. Soong, V.M. Borges, D.B. Prates, A.P. de Souza, A. Barral, J.M. Balanco, M.T. do Nascimento, E.M. Saraiva, M.A. Barcinski, Cooperation between apoptotic and viable metacyclics enhances the pathogenesis of Leishmaniasis, PLoS One 4 (2009) e5733, , http://dx.doi.org/10.1371/journal.pone.0005733.
[23] M. Duszenko, K. Figarella, E.T. Macleod, S.C. Welburn, Death of a trypanosome: a selfish altruism, Trends Parasitol. 22 (2006) 536–542, http://dx.doi.org/10.1016/j.pt.2006.08.010.
[24] M. Doroodgar, M. Delavari, M. Doroodgar, A. Abbasi, A.A. Taherian, A. Doroodgar, Tamoxifen induces apoptosis of leishmania major promastigotes in vitro, Korean J. Parasitol. 54 (2016) 9–14, http://dx.doi.org/10.3347/kjp.2016.54.1.9.
[25] S.C.S. Petri e Silva, F. Palace-Berl, L.C. Tavares, S.R.C. Soares, J.A.L. Lindoso, Effects of nitro-heterocyclic derivatives against Leishmania (Leishmania) infantum promastigotes and intracellular amastigotes, Exp. Parasitol. 163 (2016) 68–75, http://dx.doi.org/10.1016/j.exppara.2016.01.007.
[26] E.S. Yamamoto, B.L.S. Campos, J.A. Jesus, M.D. Laurenti, S.P. Ribeiro, E.G. Kallás, M. Rafael-Fernandes, G. Santos-Gomes, M.S. Silva, D.P. Sessa, J.H.G. Lago, D. Levy, L.F.D. Passero, The effect of ursolic acid on Leishmania (Leishmania) amazonensis is related to programed cell death and presents therapeutic potential in experimental cutaneous Leishmaniasis, PLoS One 10 (2015) e0144946, , http://dx.doi.org/10.1371/journal.pone.0144946.
[27] J.P. Tardivo, A. Delgiglio, C. Deoliveira, D.S. Gabrielli, H.C. Junqueira, D.B. Tada, D. Severino, R. Defatimaturchiello, M.S. Baptista, A. Del Giglio, C.S. de Oliveira, R. de Fátima Turchiello, Methylene blue in photodynamic therapy: from basic mechanisms to clinical applications, Photodiagn. Photodyn. Ther. 2 (2005) 175–191, http://dx.doi.org/10.1016/S1572-1000(05)00097-9.
[28] Y. Lu, R. Jiao, X. Chen, J. Zhong, J. Ji, P. Shen, Methylene blue-mediated photodynamic therapy induces mitochondria-dependent apoptosis in HeLa cell, J. Cell. Biochem. 105 (2008) 1451–1460, http://dx.doi.org/10.1002/jcb.21965.
[29] R. Tixeira, S. Caruso, S. Paone, A.A. Baxter, G.H. Atkin-Smith, M.D. Hulett, I.K. Poon, Defining the morphologic features and products of cell disassembly during apoptosis, Apoptosis 22 (2017) 475–477, http://dx.doi.org/10.1007/s10495-017-1345-7.
[30] T.F. Schmidt, L. Caseli, O.N. Oliveira, R. Itri, Binding of methylene blue onto langmuir monolayers representing cell membranes may explain its efficiency as photosensitizer in photodynamic therapy, Langmuir 31 (2015) 4205–4212, http://dx.doi.org/10.1021/acs.langmuir.5b00166.
[31] I.O.L. Bacellar, C. Pavani, E.M. Sales, R. Itri, M. Wainwright, M.S. Baptista, Membrane damage efficiency of phenothiazinium photosensitizers, Photochem. Photobiol. 90 (2014) 801–813, http://dx.doi.org/10.1111/php.12264.
[32] W.R. Proto, G.H. Coombs, J.C. Mottram, Cell death in parasitic protozoa: regulated or incidental? Nat. Rev. Microbiol. 11 (2013) 58–66, http://dx.doi.org/10.1038/nrmicro2929.
[33] I.A. Rodrigues, M.M.B. Azevedo, F.C.M. Chaves, C.S. Alviano, D.S. Alviano, A.B. Vermelho, Arrabidaea chica hexanic extract induces mitochondrion damage and peptidase inhibition on Leishmania spp, Biomed. Res. Int. (2014) 985171, http://dx.doi.org/10.1155/2014/985171.
[34] M.V. Lopes, V.C. Desoti, A. de O. Caleare, T. Ueda-Nakamura, S.O. Silva, C.V. Nakamura, Mitochondria superoxide anion production contributes to geranylgeraniol-induced death in Leishmania amazonensis, Evid. Based Complement. Altern. Med. (2012) 298320, http://dx.doi.org/10.1155/2012/298320.